JOURNAL OF VIROLOGY, Dec. 1994, p. 8169–8179
0022-538X/94/$04.00+0

Vol. 68, No. 12

Genetics of Mouse Hepatitis Virus Transcription: Evidence that Subgenomic Negative Strands Are Functional Templates

MARY C. SCHAAD[1] AND RALPH S. BARIC[2,3]*

Department of Parasitology and Laboratory Practice[1] and Program in Infectious Diseases, Department of Epidemiology,[2] and Department of Microbiology and Immunology,[3] University of North Carolina at Chapel Hill, Chapel Hill, North Carolina 27599-7400

Received 11 May 1994/Accepted 31 August 1994

Mouse hepatitis virus (MHV) A59 temperature-sensitive (*ts*) mutants belonging to complementation group C were characterized and mapped by standard genetic recombination techniques. Temperature shift experiments early in infection suggested that the group C allele can be divided into two phenotypically distinct subgroups, designated C1 and C2. Since previous data indicated that the group C1 mutants probably contained an early defect which affects negative-strand synthesis, RNA synthesis was further examined by analyzing replicative-form (RF) RNA. Full-length as well as subgenomic-length RF RNAs were radiolabeled from 3 to 12 h postinfection (p.i.) and labeled late in infection after shift to the nonpermissive temperature (39.5°C). The relative percent molar ratios of each mRNA and corresponding RF RNA were roughly equivalent throughout infection. Temperature shift experiments at 5.5 or 6.0 h p.i. resulted in an 83 to 92% reduction in the amount of total RF RNA at 39.5°C. Radiolabeling time course experiments after temperature shift to 39.5°C also demonstrated incorporation (6 to 9 h p.i.) into both subgenomic-length and full-length RF RNAs, suggesting that previously transcribed negative strands were functional templates throughout infection. To determine if the reduction in RF RNA was due to a decrease in positive- or negative-strand RNA synthesis, rates of mRNA synthesis were calculated from both full-length and subgenomic-length templates. The rate of mRNA synthesis after the shift was increased at 39.5°C compared with that at 32°C regardless of the template used; however, transcription rates calculated from subgenomic-length templates were similar to those of other viral and eukaryotic polymerases. These findings support the notion that the group C1 allele regulates negative-strand RNA synthesis and strongly suggest that the subgenomic negative-strand RNAs are probably the predominant functional templates for the synthesis of positive-strand RNAs late in infection.

The genome of mouse hepatitis virus (MHV), a coronavirus, consists of an approximately 31-kb single-stranded plus-polarity RNA (19, 23, 29). Replication of genomic RNA occurs through a negative-strand RNA intermediate and results in the synthesis of six or seven subgenomic mRNAs as well as additional progeny genomic RNA (34, 38, 40). The mRNAs are arranged in a 3′-coterminal nested set and contain a 5′-end leader RNA sequence of approximately 70 nucleotides that is derived from the 5′ end of the genome and is fused to mRNA at highly conserved intergenic sequences [UC(U/C)AAAC] (4, 6, 8, 15, 40). During mixed infection, leader RNA sequences from one strain of MHV are joined to the subgenomic mRNAs of heterologous MHV strains (28, 44). Heterogeneity can also occur at the leader-body fusion sites, as well as in less-than-perfect intergenic sequences that can function as transcriptional start sites for mRNA synthesis (17, 25, 27, 34, 38, 42). Both full-length and subgenomic-length negative-strand RNAs and replicative-form (RF) RNAs have been detected in coronavirus-infected cells including porcine transmissible gastroenteritis virus, bovine coronavirus, and MHV (11, 33, 34, 37).

Several discontinuous-transcription models have been proposed to explain the presence of leader RNAs on positive-strand RNAs and antileader RNAs on full-length and subgenomic-length negative-strand RNAs (15, 33, 36, 40). It has been suggested that transcription may occur in two phases: an early, primary phase in which subgenomic-length mRNA is first synthesized from a full-length template, and a secondary phase in which it is synthesized from a subgenomic-length template (13, 23, 33, 37, 43). One model proposes that subgenomic mRNA is initially synthesized from a full-length negative-strand template by a leader-priming mechanism followed by mRNA amplification through a subgenomic negative-strand intermediate (4, 37). This model is consistent with results of leader reassortant studies and also of UV transcriptional mapping studies, which suggest that early in MHV infection the production of genome-length and subgenomic-length mRNA is inhibited at equivalent UV doses (28, 43). While it is clear from nascent-labeling experiments that subgenomic-length replicative-intermediate (RIs) are transcriptionally active (33), it has been suggested that these subgenomic RIs may represent dead-end transcriptional products involved in the synthesis of a single mRNA (13).

Alternative models propose that subgenomic-length negative strands are synthesized directly from the genomic template, either by a looping out or splicing mechanism or by transcription attenuation within intergenic regions, to provide the template for subsequent mRNA synthesis (33). Currently, the looping-out mechanism is less attractive since it has not been demonstrated that full-length RIs can be degraded into subgenomic RF RNA (3, 33).

In this study, *ts* mutants defective in negative-strand synthesis were used to study the synthesis and function of the full-length versus subgenomic-length RNA in MHV-infected cells. Our data provide strong genetic support for the hypothesis that subgenomic negative-stranded RNAs are the predominant functional templates for the synthesis of subgenomic mRNAs late in infection (33, 36, 37).

* Corresponding author. Mailing address: Department of Epidemiology, University of North Carolina at Chapel Hill, CB 7400, Chapel Hill, NC 27599-7400. Phone: (919) 966-3895. Fax: (919) 966-2089.

MATERIALS AND METHODS

Virus, cell lines, and recombination mapping. MHV A59 *ts* mutants (NC1, NC3, NC10, and LA9) belonging to RNA$^-$ complementation group C were used in this study (35). Complementation indices among the group C mutants were determined as previously described (35). Revertants of LA9 and NC3 were obtained by isolating plaques that initially grew at 39.5°C and which maintained the ability to grow at restrictive temperatures after successive plaque assays, as previously described (9). Mutants and revertants were propagated in DBT cells, a murine astrocytoma cell line, in Dulbecco's modified minimum essential medium (DMEM) containing 10% Nu-serum (Irvine Scientific) and 1% gentamicin–kanamycin (35). The 17CL1 cells (kindly provided by Stanley Sawicki) were maintained in DMEM containing 6% fetal calf serum, 5% tryptose phosphate broth, and 1% penicillin–streptomycin. To reduce fusion of the 17CL1 cells during infection, medium at pH 6.8 was used as previously described (32).

Recombination analyses, measuring the percentage of *ts*$^+$ progeny virus present following a genetic cross at the permissive temperature, were performed as previously described (2). Recombination frequencies are presented as mean ± standard deviation from at least three independent assays.

Virus growth curves. Growth curves for NC1, NC3, NC10, LA9, and LA9-Rev2 (revertant no. 2) were determined as previously described (35). Briefly, cultures were infected at a multiplicity of infection (MOI) of 10 at the permissive temperature (32°C) and maintained at this temperature until 5 h postinfection (p.i.), when half the cultures were shifted up to 39.5°C. Virus progeny were harvested at 2, 5, 7, 9, 11, and 14 h p.i. for analysis by plaque assay. At the indicated times p.i., intracellular RNA was harvested and equivalent amounts were bound to nitrocellulose filters, probed with strand-specific RNA probes, and quantified as previously described (35).

Radiolabeling and isolation of viral RNA. Viral RNAs were radiolabeled in DBT or 17CL1 cells. After infection, cultures were overlaid with complete DMEM for DBT cells or pH 6.8 DMEM for 17CL1 cells and incubated at 32°C. At least 30 min prior to the addition of radioisotope, the cultures were treated with actinomycin D (Sigma) at concentrations ranging from 2.5 to 10 μg/ml. Higher concentrations of actinomycin D were used in $^{32}P_i$-labeling experiments to reduce radiolabeling of host cell RNA and DNA. [^{3}H]uridine (Amersham) at 100 μCi/ml (for mRNA labeling only) or 300 μCi/ml (for analysis of RF RNAs) was added to virus-infected cultures at different times p.i. for 2 h as indicated in the figure legends. For labeling with $^{32}P_i$ (ICN), cultures of 17CL1 cells were grown overnight in 90% phosphate-free MEM (Gibco) containing 10% fetal calf serum and then 300 μCi of radiolabel per ml was added to the cultures at different times p.i. in 100% phosphate-free MEM. All viral RNA was extracted as described elsewhere (33).

Analysis of viral RNA. Viral mRNA and RF RNA were analyzed by the method described by Sawicki and Sawicki (33). Briefly, RNA was treated with 10 U of DNase I (Boehringer Mannheim) in 1× DNase buffer (500 mM NaCl, 50 mM Tris [pH 7.8], 10 mM $CaCl_2$, 10 mM $MgCl_2$) for 15 min at 30°C. One-sixth of the total RNA was set aside to be heat denatured at 90°C and analyzed as mRNA, while the remaining five-sixths of the sample was analyzed as RF RNA and digested with 50 ng of RNase A (Sigma) per ml in 1× RNase buffer (700 mM NaCl, 10 mM Tris [pH 7.4], 30 mM EDTA) for an additional 15 min at 30°C. The RNA was electrophoresed on 1× Tris-borate-EDTA (TBE)–0.8% agarose gels, soaked in Enlightening (Dupont NEN) if ^{3}H labeled, and dried under vacuum before exposure to Hyperfilm-MP (Amersham) at −70°C. Dried gels containing $^{32}P_i$-labeled viral RNAs were scanned for 10 to 12 h by the AMBIS radioanalytic imaging system (Ambis, San Diego, Calif.). The relative percent molar ratios of mRNA and RF RNA were calculated as previously described (18, 19).

Calculation of rates of mRNA synthesis. Total counts per minute (cpm) obtained by the AMBIS radioanalytic imaging system were corrected for background signal, resulting in net cpm. The net cpm value was then corrected for sample volume loaded onto gels; i.e., mRNA counts were multiplied by 6, and RF counts were multiplied by 6/5. To determine whether rates of mRNA synthesis were affected by the *ts* lesion in NC3, rates of transcription were calculated by assuming that either a full-length or a same-sized negative-strand template functioned exclusively in mRNA synthesis. This was necessary since the actual template for mRNA synthesis late in infection is controversial (1, 13, 33, 37, 44). Calculations to determine the time required to transcribe an MHV mRNA from a same-sized subgenomic-length RF template were based on the general formula used for Sindbis (SB) virus (3, 39). This was probably a valid assumption since the rates of SB virus 42S or 26S RNA synthesis were also calculated from distinct same-sized RF RNA templates, i.e., RFI or RFIII, respectively (3, 39). Assuming that positive-strand RNA is preferentially labeled from the subgenomic-length template (33), the formula to calculate the time of synthesis of one mRNA from one subgenomic-length RF template (T_A) is: $T_A = T/(A/B)$, where T is the labeling time (60 min), A is a particular mRNA cpm, and B is the cpm from its corresponding-length RF RNA (3, 39).

The above formula is valid only if subgenomic negative strands are not transcriptionally dead-end products involved in the synthesis of a single positive strand (13). If this is the case, the "leader-primed" transcription model dictates that all viral mRNAs will be transcribed from a full-length RI, predicting that only that portion of the full-length RI that is equivalent to the size of a given mRNA functions in the synthesis of that mRNA. The nested-set structure of the MHV mRNAs further dictates that nascent positive strands destined to become each viral mRNA will also be present on the full-length RI (4). Thus, to calculate the rate of mRNA synthesis, assuming that only leader-primed transcription from full-length RI templates was functioning, we modified and substituted B in the above formula to correct for (i) the portion of the full-length RF RNA that could be contributing to the synthesis of a particular subgenomic mRNA, ($C(D/E)$ (see below), and (ii) the ratio of nascent positive strands synthesized from this portion of the RF RNA (A/F). As predicted from the leader-primed transcription model (4), we have assumed that the ratio of nascent positive strands on the full-length RIs (A/F) should reflect the final ratio of a given mRNA (A) to all mRNA transcribed during the labeling period (F). Since mRNAs do not arise spontaneously but, rather, originate as nascent positive strands on RI RNAs, it is a valid assumption that the ratio of nascent positive-strand RNAs on the RI RNA will reflect the final ratio of each mRNA during transcription (4, 30, 39). Thus, B in the original formula is substituted with $(C)(D/E)(A/F)$, and the final formula can be mathematically expressed as: $T_A = (T)(C)(D/E)(A/F)/A$, where T is the labeling time (60 min), C is the RF1 cpm, D is the portion of the full-length template contributing to the synthesis of a selected mRNA and is equivalent to the size of the particular mRNA (in kilobases), E is the size of a full-length negative-strand RNA (31 kb), A is the selected mRNA cpm, and F is the total cpm of all mRNAs.

TABLE 1. Virus titers of the group C mutants and revertants

Mutant	Virus titer at:		Reversion frequency
	32°C	39.5°C	
NC3	3.8×10^7	1.0×10^3	2.6×10^{-5}
NC10	9.3×10^7	1.0×10^2	1.2×10^{-6}
NC1	7.4×10^7	1.0×10^2	1.4×10^{-6}
LA9	8.6×10^7	7.8×10^3	9.0×10^{-5}
LA9Rev1	2.9×10^7	1.0×10^7	3.4×10^{-1}
LA9Rev2	4.0×10^7	1.4×10^7	3.5×10^{-1}
NC3Rev1	1.0×10^8	7.0×10^7	7.0×10^{-1}
NC3Rev2	1.0×10^8	7.0×10^7	7.0×10^{-1}

To calculate putative polymerase rates during infection, we converted the time (in minutes) required to transcribe mRNAs 7, 6, 3, and 1 to nucleotides per minute by dividing the time to transcribe a given mRNA into the size (in nucleotides) of the respective mRNA. Comparisons among calculations assume that there are roughly equivalent amounts of RNA polymerase and template RNAs and roughly equivalent mRNA decay rates at different times p.i. Statistics, including mean ± standard deviation and *T* test, were calculated by the Statworks (version 1.2) program (Cricket Software, Inc., Philadelphia, Pa.).

RESULTS

Genetic mapping and phenotypic characterization of the complementation group C mutants. We have previously shown that at least one group C mutant (LA9) continues to synthesize mRNA and release infectious virus after temperature shift to 39.5°C. Using strand-specific RNA probes, negative-strand RNA synthesis did not increase significantly after the shift, suggesting that the group C allele probably encodes an early function affecting negative-strand synthesis (35). Table 1 shows the titers and the reversion frequencies of the group C mutants used in these studies. In support of previous complementation data and RNA recombination mapping data (2, 9, 35), complementation data and detailed recombination mapping studies among the group C mutants demonstrated that the *ts* alleles were closely linked (Table 2).

Prior studies with alphaviruses have demonstrated that more than one phenotypically distinct function may be represented within a single complementation group (30). To determine if phenotypically distinct subgroups exist within the group C mutants, cultures of cells were infected with different mutants and shifted to the restrictive temperature at 5 h p.i. Samples were taken at different times p.i. for infectious-virus analysis by plaque assay (Fig. 1). In contrast to LA9 and NC3, which continue to release infectious virus after the shift, the replication of NC10 and NC1 was significantly inhibited in the ability to produce infectious virus. To determine if the block in NC1 and NC10 was linked to the inability to transcribe mRNA, intracellular RNA was isolated at different times after the shift, bound to nitrocellulose filters, and probed with strand-specific RNA probes that detect all viral mRNAs (Fig. 2) (35). While preliminary, these results suggest that the group C *ts* mutants can be subdivided into two phenotypically distinct subgroups. The subgroup C1 mutants, represented by NC3 and LA9, continue to release infectious virus and synthesize significant quantities of mRNA at 39.5°C after the temperature shift at 5 h p.i. The slight delay in PFU production at 39.5°C was probably due to a slight delay in the accumulation of viral mRNA. In contrast, the subgroup C2 mutants, NC1 and NC10, do not release infectious virus and synthesize little if any mRNA at 39.5°C after the temperature shift at 5 h p.i. (Fig. 1 and 2). The LA9 and NC3 revertants transcribe mRNA and produce infectious virus at the restrictive temperature (data not shown), typical of all the MHV A59 revertants isolated to date (9). We focused our efforts on the group C1 mutants since previous studies suggested that they contain a defect in negative-strand RNA synthesis at the restrictive temperature (35).

Effect of early and late temperature shift on NC3 mRNA and RF RNA synthesis. If subgenomic negative-strand RNAs are functional templates for mRNA synthesis, subgenomic RF RNAs should be detected throughout infection. We performed a time course experiment of NC3 mRNA and RF RNA synthesis at 32°C and after radiolabeling with [^{3}H]uridine at 2-h intervals between 6 to 8, 8 to 10, and 10 to 12 h p.i. (Fig. 3). To verify that the *ts* lesion was present in an allele which functions early in infection, we also shifted virus-infected cells to the nonpermissive temperature late (9 h p.i.) in infection, 1 h prior to adding label. Genome-length as well as all subgenomic-length mRNAs and RF RNAs were detectable throughout the time course of the experiment (6 to 12 h p.i.). Moreover, a temperature shift late in infection had no effect on positive-strand synthesis, as NC3 mRNA and RF RNA synthesis was essentially the same at both 32 and 39.5°C from 10 to 12 h p.i. (Fig. 3). As previously described, an eighth mRNA and its corresponding RF RNA, which are encoded at the 3′ end of the viral genome, were also detected on occasion (34).

If the group C1 mutants were defective in the ability to synthesize negative-strand RNA after the shift, a corresponding reduction in RF RNA should be seen in cultures shifted earlier in infection. 17CL1 cells were infected with NC3 and shifted to the restrictive temperature at 6 h p.i. The viral RNA was radiolabeled with $^{32}P_i$ from 6.5 to 9 h p.i. Following the temperature shift, NC3 full-length as well as subgenomic-length mRNA and RF RNA were prevented from increasing to maximal levels as detected at the permissive temperature (Fig. 4). AMBIS radioanalytic imaging system scans indicated that after the shift to 39.5°C, NC3 total RF RNA and mRNA levels were reduced by approximately 92 and 49%, respectively, relative to those of controls maintained at 32°C.

Time course of RF RNA synthesis after the temperature shift. If subgenomic negative strands are dead-end transcriptional products and the group C1 mutants transcribe little new

TABLE 2. Genetic recombination frequencies and complementation indices among the group C mutants

Mutant	Recombination frequency[a] (complementation index) for:				
	LA9	NC10	NC3	NC1	LA7
LA9		0.20 ± 0.05 (0.1)	0.10 ± 0.09 (0.8)	0.65 ± 0.63 (3.0)	4.45 ± 0.85 (34.2)
NC10			0.79 ± 0.20 (0.8)	0.08 ± 0.005 (0.5)	4.85 ± 1.00 (45.0)
NC3				0.47 ± 0.22 (0.1)	3.74 ± 2.30 (250.0)
NC1					3.65 ± 2.30 (129.2)
LA7					

[a] Mean ± standard deviation.

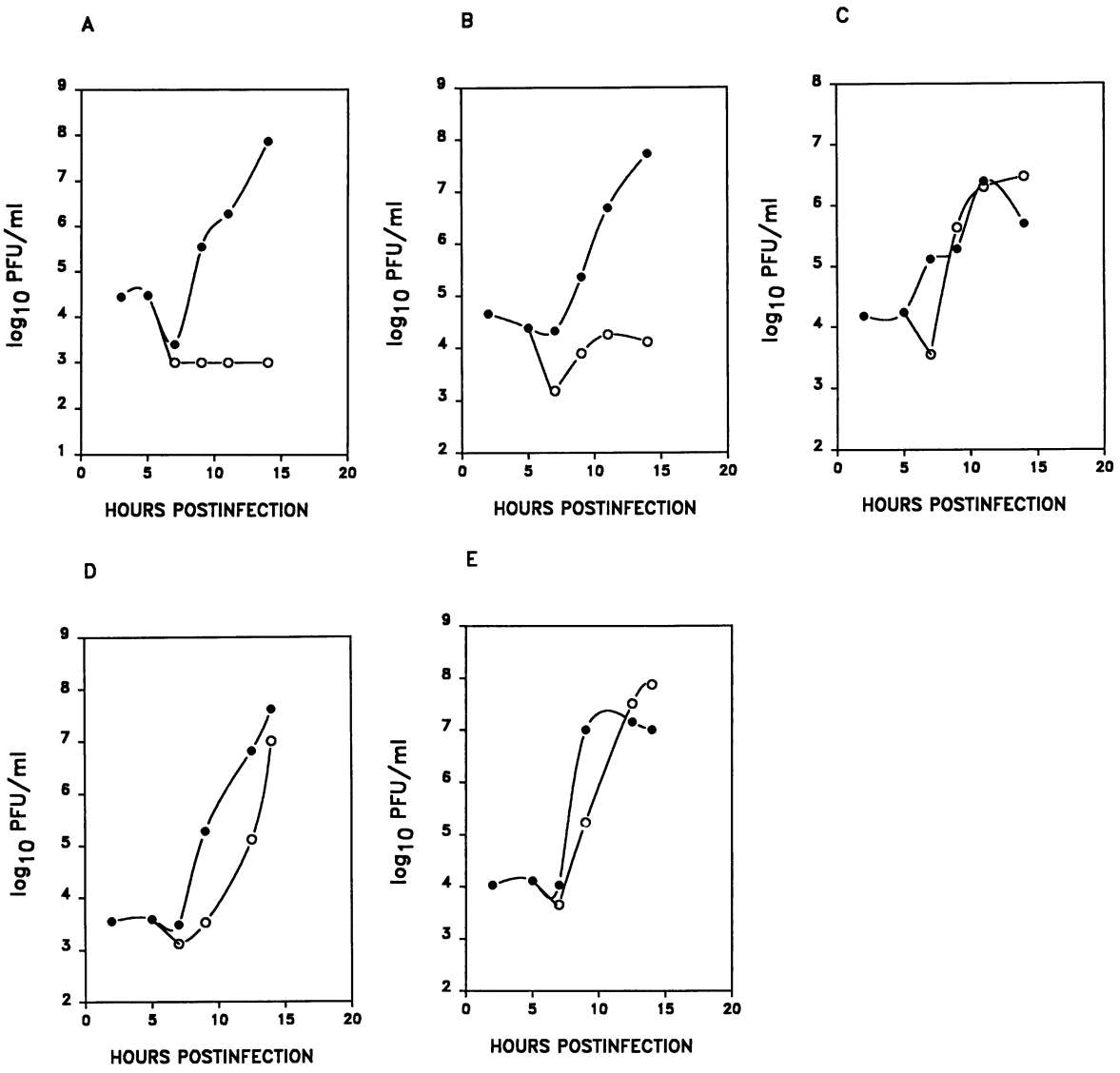

FIG. 1. Growth curves of the group C mutants. Infection was initiated at 32°C, and at 5 h p.i. half the cultures were shifted to 39.5°C. Infectious virus was analyzed by plaque assay. (A) NC1; (B) NC10; (C) NC3; (D) LA9; (E) LA9-Rev2. Symbols: ●, 32°C; ○, 39.5°C.

negative-strand RNA after the temperature shift (35), a decrease in $^{32}P_i$ incorporation into the subgenomic-length but not full-length RFs at 39.5°C should be evident over time as the preexisting subgenomic templates transcribe a single positive strand and burn out. This should also result in an alteration in the relative percent molar ratio of full-length to subgenomic-length RF RNAs after the shift. We analyzed the kinetics of NC3 and NC3-Rev2 RF RNA synthesis at 32 and 39.5°C from 4 to 9 h p.i. Infected cultures were shifted at 5.5 h p.i. and radiolabeled with $^{32}P_i$ from 6 to 7, 7 to 8, and 8 to 9 h p.i. (Fig. 5). Consistent with previous studies, very little mRNA and RF RNA were observed with both NC3 and NC3-Rev2 at 4 and 5 h p.i. in cultures maintained at 32°C (35). NC3-Rev2 mRNA and RF RNA synthesis increased later in the infection and peaked by 8 to 9 h p.i. at 32°C and by 7 h p.i. at 39.5°C (Fig. 5C and D). With NC3 at 32°C, synthesis of full-length and subgenomic-length RF RNA rapidly increased between 7 and 9 h p.i. (Fig. 5B). At 39.5°C after the temperature shift at 5.5 h p.i., a reduction in the amount of NC3 full-length and subgenomic-length RF RNA and mRNAs was observed at each labeling period compared with that in the controls (Fig. 5A and B).

To quantitatively determine the levels of mRNA and RF RNA synthesized after the temperature shift, the four $^{32}P_i$-labeled gels shown in Fig. 5 were scanned by the AMBIS radioanalytic imaging system. Figure 6 is a graphic representation of the net cpm for NC3 and NC3-Rev2 mRNA and RF RNA. As expected, the numbers reflect nearly constant levels of total mRNA and RF RNA synthesis in NC3-Rev2 after the temperature shift (Fig. 6B). In contrast, by 9 h p.i., NC3 total RF RNA synthesis did not increase significantly and was reduced by 83% compared with that in controls maintained at the permissive temperature (Fig. 6A). While the *ts* defect in NC3 also resulted in nearly equivalent reductions in the amount of radiolabel incorporated into both RF1 and RF7 after shift (Fig. 6C), the amount of radiolabel incorporated into NC3 subgenomic-length and full-length RF RNA slowly

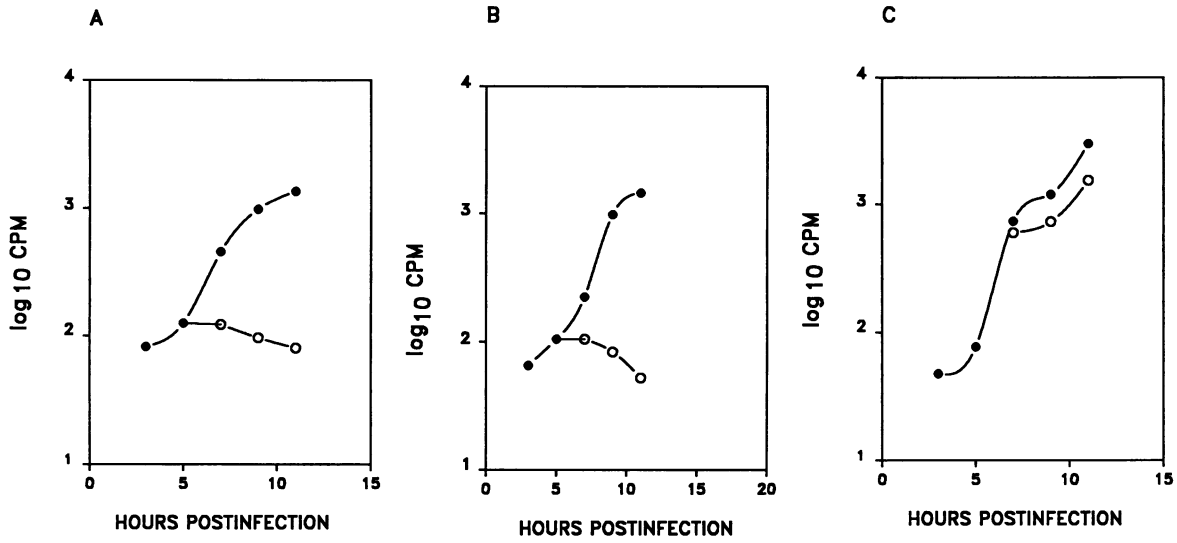

FIG. 2. RNA synthesis in the group C mutants. Infection was initiated in DBT cells infected at a MOI of 10 with each *ts* mutant. At 5.0 h p.i., half of the cultures were shifted to 39.5°C and intracellular RNA was isolated as described in Materials and Methods. Equivalent amounts of RNA were bound to nitrocellulose filters and probed with strand-specific RNA probes that detect all MHV mRNAs. The bands were visualized, excised, and counted. (A) NC1; (B) NC10; (C) LA9. Symbols: ●, 32°C; ○, 39.5°C.

increased at 39.5°C over time, clearly indicating that the negative-strand templates were not depleted.

We also calculated the percent molar ratio of RF1 through RF7 after the shift to the restrictive temperature and in control cultures maintained at the permissive temperature (Table 3). These data clearly demonstrated that the percent molar ratios of RF1 through RF7 reflected the molar ratios of their respective mRNAs and remained relatively constant after the shift, indicating that the subgenomic RF RNAs are transcriptionally active and are not dead-end transcription products.

Previous UV kinetic studies demonstrated that at 2.5 h p.i. and 37°C, most of the MHV mRNAs (>80%) have a target size larger than their respective RNA size (43). We performed early temperature shift experiments to determine whether primary and secondary transcription could be uncoupled. NC3-infected cultures were shifted at 1.5 and 3.0 h p.i. and labeled with 500 μCi/ml of [^{3}H]uridine per ml from 3 to 4 or 4 to 5 h p.i., respectively. In agreement with earlier studies, viral mRNA and RF RNA synthesis was significantly reduced when cultures were shifted to the restrictive temperature at earlier times p.i. (35). In cultures shifted at 1.5 h p.i., radiolabel was

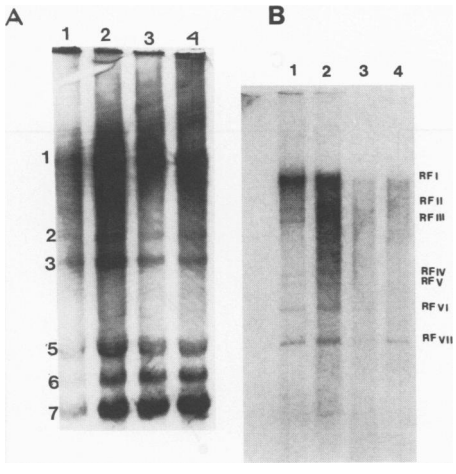

FIG. 3. Time course of [^{3}H]uridine labeling of N3 mRNA and RF RNA after a late shift. DBT cells were infected with NC3 at an MOI of 6 and treated with actinomycin D 0.5 h before being labeled. Viral mRNA and RF RNA were labeled at 100 and 300 μCi/ml for 2-h periods at 32°C at the times indicated below. At 9 h p.i., half the cultures were shifted to the restrictive temperature. (A) mRNA (24-h exposure); (B) RF RNA (60-h exposure). Lanes: 1, 6 to 8 h p.i. 32°C; 2, 8 to 10 h p.i., 32°C; 3, 10 to 12 h p.i., 32°C; 4, 10 to 12 h p.i., 39.5°C.

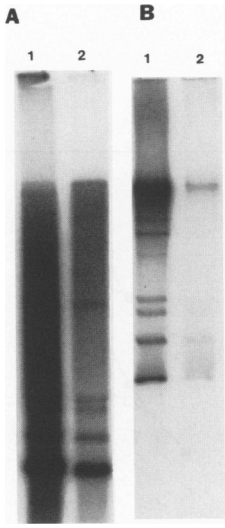

FIG. 4. $^{32}P_i$ labeling of NC3 mRNA and RF RNA after an early shift. 17CL1 cells were infected with NC3 at an MOI of 10 and treated with actinomycin D at 5 h p.i. At 6 h p.i., half the cultures were shifted to 39.5°C. Viral RNA was radiolabeled from 6.5 to 9 h p.i. with 300 μCi of $^{32}P_i$ per ml and extracted at 9 h p.i. (A) mRNA; (B) RF RNA. Lanes: 1, 32°C; 2, 39.5°C.

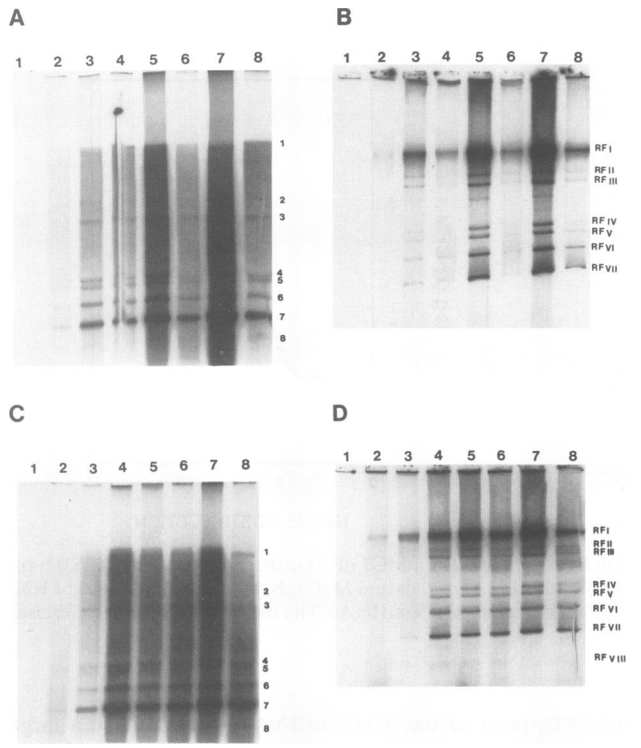

FIG. 5. Time course of $^{32}P_i$ labeling of NC3 and NC3-Rev2 mRNA and RF RNA. 17CL1 cells were infected with either mutant or revertant at an MOI of 10 and treated with actinomycin D at least 1 h before being labeled. The infection was initiated at the permissive temperature, and at 5.5 h p.i. half the cultures were shifted to the nonpermissive temperature. Viral RNA was labeled for 1-h periods at various times postinfection with $^{32}P_i$ at 300 μCi/ml, and the RNA was extracted at the times indicated below. (A) NC3 mRNA; (B) NC3 RF RNA; (C) NC3-Rev2 mRNA; (D) NC3-Rev2 RF RNA. Lanes: 1, 4 h p.i.; 2, 5 h p.i.; 3, 7 h p.i., 32°C; 4, 7 h p.i., 39.5°C; 5, 8 h p.i., 32°C; 6, 8 h p.i., 39.5°C; 7, 9 h p.i., 32°C; 8, 9 h p.i., 39.5°C.

incorporated into the smaller subgenomic mRNAs, but we could not clearly detect significant label in any viral RF RNAs. By 3 h p.i., label was incorporated into both full-length and subgenomic-length mRNA and RF RNA, indicating that both full-length and subgenomic-length negative-strand RNAs were transcriptionally active at very early times p.i. (Fig. 7).

Time required to transcribe NC3 mRNA after the temperature shift. The defect in NC3 transcription resulting in a reduction in the amount of radiolabeled RF RNA after shift could be due to a decrease in negative- and/or positive-strand RNA synthesis. For the positive-stranded RNA viruses, it is understood that viral mRNA is transcribed from a complementary negative-strand RNA. Nascent viral RNA is located in the RI RNA, and following RNase digestion, much of the recently transcribed RNA remains affiliated with double-stranded RF RNA cores. Consequently, the rate at which label is incorporated into RF RNAs should be a direct measure of the rate of single-stranded RNA synthesis from its template (3, 4, 31, 33, 36, 37, 39). In an attempt to definitively distinguish between the two possible defects in NC3, we calculated the rates of mRNA synthesis by using the formula developed for SB virus (3, 39). Rate calculations for SB virus with pulse-labeling periods from only a few minutes to 2 h have been studied. Only minor variations in the times required to transcribe a given mRNA from its equivalent same-sized template have been noted (3, 39). For MHV, which has template RNAs ranging from 1.7 to 32 kb (33), the longer radiolabeling times (1 h) used in these studies would ensure that all of the RIs would be fully saturated with label, providing a more accurate estimate of the time required to synthesize a given mRNA from its template (39). If mRNA degrades or if negative-stranded RNA is also radiolabeled during the labeling period, our findings would probably represent the upper limit on the time required to transcribe a given mRNA from its particular template (39).

Since our previous results corroborated studies by other laboratories and indicated that subgenomic negative strands were functional templates throughout infection (33, 36, 37), we addressed the question by calculating the rates of mRNA 1, 3, 6, and 7 synthesis from 6 to 7, 7 to 8, and 8 to 9 h p.i., assuming that the predominant template for mRNA synthesis was its

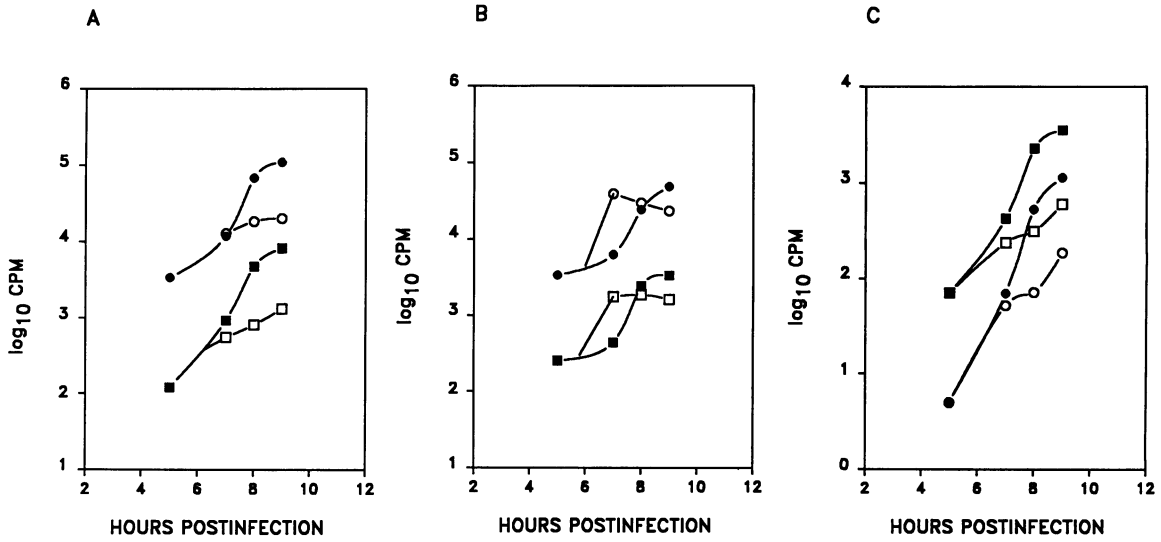

FIG. 6. Effect of temperature shift on mRNA and RF RNA synthesis. Corrected net cpm for NC3 (A), NC3-Rev2 (B), and NC3 RF1 versus RF7 (C) are shown. Symbols for panels A and B: ●, mRNA at 32°C; ○, mRNA at 39.5°C; ■, RF RNA at 32°C; □, RF RNA at 39.5°C. Symbols for panel C: ■, RF1 at 32°C, □, RF1 at 39.5°C; ●, RF7 at 32°C; ○, RF7 at 39.5°C.

TABLE 3. Relative percent molar ratio of full-length and subgenomic-length mRNA and RF RNA after the shift

Viral RNA species	Mol wt of mRNA	Relative % molar ratio[a] (n = 3) of:							
		RF RNA (32°C)		RF RNA (39°C)		mRNA (32°C)		mRNA (39.5°C)	
		NC3	NC3-Rev2	NC3	NC3-Rev2	NC3	NC3-Rev2	NC3	NC3-Rev2
1	~9.79 × 10^6	8.8 ± 1.2	9.0 ± 0.2	7.3 ± 0.8	5.8 ± 0.2	0.70 ± 0.2	0.8 ± 0.2	1.21 ± 0.6	0.50 ± 0.2
2	3.04 × 10^6	8.2 ± 1.9	10.9 ± 2.1	6.1 ± 1.6	6.6 ± 0.7	4.6 ± 0.5	4.9 ± 0.8	5.9 ± 0.9	3.3 ± 0.8
3	2.40 × 10^6	8.3 ± 0.9	10.3 ± 1.7	6.0 ± 0.9	8.0 ± 1.2	6.9 ± 0.8	6.6 ± 0.8	7.0 ± 0.3	5.0 ± 0.8
4	1.15 × 10^6	8.5 ± 0.6	7.5 ± 1.5	9.9 ± 2.0	7.1 ± 1.1	11.7 ± 0.5	10.7 ± 0.5	10.5 ± 1.3	9.8 ± 1.8
5	1.0 × 10^6	10.3 ± 1.2	9.8 ± 1.0	13.8 ± 2.8	9.6 ± 0.7	13.7 ± 2.4	13.3 ± 1.2	12.5 ± 2.4	13.7 ± 1.2
6	0.81 × 10^6	19.8 ± 1.5	16.3 ± 0.8	24.5 ± 3.1	20.0 ± 2.2	17.2 ± 1.3	16.7 ± 1.5	16.4 ± 2.3	18.1 ± 2.3
7	0.56 × 10^6	36.0 ± 6.9	36.2 ± 5.7	33.0 ± 7.8	42.7 ± 1.3	45.4 ± 0.9	46.8 ± 1.7	46.3 ± 4.5	48.8 ± 5.3

[a] Mean ± standard deviation.

same-sized subgenomic RI template (or, for mRNA 1, RI 1) (Table 4) (3, 32, 37, 39). Appropriately, the times required to transcribe mRNA from a corresponding subgenomic-length template increased with increasing size of the mRNA and at 32°C were roughly equivalent between NC3 and NC3-Rev2. Although some variability was evident, especially in the times required to transcribe genomic RNA, this was probably due to minor amounts of degradation following extraction and from the packaging and release of genome-length RNAs in progeny virions. Less time was required to synthesize equivalent-sized mRNA at 39.5°C than at 32°C for both NC3 and NC3-Rev2, indicating that positive-strand synthesis was not significantly inhibited in NC3-infected cultures after the temperature shift.

We also calculated rates of mRNA synthesis, assuming that only the full-length template was functional and mRNA synthesis occurred by leader-primed transcription (4). The leader-primed transcription model proposes that only the portion of the full-length RI equivalent to the size of a given mRNA contributes to the synthesis of that mRNA. The model also proposes that the ratio of nascent positive strands on the RI RNA (or the rate of synthesis of a given mRNA) is dictated by leader priming from unique intergenic start sites. Consequently, the ratio of the nascent positive strand of each mRNA on the RI RNA will directly determine the final ratio of each mRNA transcribed throughout infection (4). The complexity of a full-length RI transcribing subgenomic mRNA by leader-primed transcription has required a significant modification of the standard formula (see Materials and Methods). As with the previous calculations, the times were comparable between NC3 and NC3-Rev2 at 32°C, with more time required to synthesize larger mRNAs (Table 5). Synthesis was also increased at 39.5°C compared with 32°C for NC3 and its revertants, demonstrating that the defect in NC3 did not affect the rate of positive-strand RNA synthesis. However, the time required to synthesize any mRNA from the full-length template was drastically reduced compared with that from the subgenomic-length template, indicating that mRNA synthesis must be extremely efficient if it is derived only from a full-length RI.

To investigate the statistical significance of the increased rates of mRNA synthesis following the shift to 39.5°C with NC3, we calculated the average rate (in nucleotides per minute) of RNA transcription at 32 and 39.5°C from mRNAs 1, 3, 6, and 7 at 6 to 7, 7 to 8, and 8 to 9 h p.i., assuming that a same-sized template was functional (Table 6). No significant differences (n = 12) were detected in the rate of transcription between NC3 and NC3-Rev2 at 32°C, assuming that either a

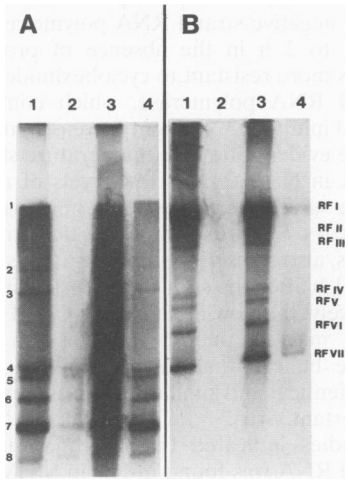

FIG. 7. NC3 mRNA and RF RNA synthesis after an early temperature shift. 17CL1 cells were infected with NC3 at an MOI of 10 for 1 h. At 1.5 and 3.0 h p.i., half of the cultures were shifted to the restrictive temperature and radiolabeled with 500 μCi of [^{3}H]uridine per ml from 4 to 6 h p.i. The radiolabeled RNAs were separated on 0.8% agarose gels, soaked in Enlightening, and exposed to film for 36 days. (A) NC3 mRNA. Lanes: 1, NC3 mRNA from 3 to 4 h p.i. at 32°C; 2, NC3 mRNA after the shift at 1.5 h to 39.5°C and labeled from 3 to 4 h p.i.; 3 NC3 mRNA from 4 to 5 h p.i. at 32°C; 4, NC3 mRNA after a shift at 3.0 h to 39.5°C and labeled from 4 to 5 h p.i. (B) NC3 RF RNA. Lanes: 1, NC3 RF RNA at 3 to 4 h p.i.; 2, NC3 RF RNA after the shift at 1.5 h to 39.5°C and labeled from 3 to 4 h p.i.; 3, NC3 RF RNA at 4 to 5 h p.i.; 4, NC3 RF RNA after the shift at 3.0 h to 39.5°C and labeled from 4 to 5 h p.i.

TABLE 4. Putative times required to transcribe mRNA from subgenomic replicative intermediates at the permissive and restrictive temperatures

mRNA species	Time (min) for transcription at:			
	Permissive temp		Restrictive temp	
	6–7 h p.i.	7.8 h p.i.	6–7 h p.i	7–8 h p.i.
NC3 mRNA7	1.45	1.92	1.09	1.01
NC3 mRNA6	2.80	2.75	1.93	2.75
NC3 mRNA3	3.32	2.80	1.61	1.53
NC3 mRNA1	27.00	23.70	10.90	17.20
NC3-Rev2 mRNA7	1.38	2.55	1.46	2.05
NC3-Rev2 mRNA6	2.22	2.54	1.90	2.54
NC3-Rev2 mRNA3	3.52	4.93	2.21	3.45
NC3-Rev2 mRNA1	25.00	42.40	13.60	26.90

TABLE 5. Time required for the synthesis of MHV mRNAs from a full-length negative-strand RNA template

mRNA species	Time (min) for mRNA synthesis at:			
	Permissive temp		Restrictive temp	
	6–7 h p.i.	7–8 h p.i.	6–7 h p.i.	7–8 h p.i.
NC3 mRNA 7	0.13	0.17	0.07	0.05
NC3 mRNA 6	0.17	0.16	0.09	0.08
NC3 mRNA 3	0.56	0.52	0.29	0.26
NC3 mRNA 1	2.15	1.99	1.11	1.02
NC3-Rev2 mRNA 7	0.10	0.16	0.06	0.10
NC3-Rev2 mRNA 6	0.13	0.21	0.08	0.11
NC3-Rev2 mRNA 3	0.46	0.70	0.25	0.38
NC3-Rev2 mRNA 1	1.76	2.67	1.00	1.48

subgenomic-length ($P = 0.93$) or full-length ($P = 0.81$) template was preferentially functional. However, a significant increase in the rate of mRNA synthesis from a subgenomic-length template was evident after the shift to 39.5°C with NC3 ($P < 0.05$) but not with NC3-Rev2 ($P = 0.57$).

Assuming that only a full-length RI was acting as a functional template, significant increases in the rate of transcription were evident with both NC3 and NC3-Rev2 after the shift to 39.5°C ($P < 0.001$). These data demonstrate that the rate of NC3 mRNA synthesis after the shift is increased at 39.5°C compared with 32°C regardless of the template used, and they strongly suggest that the defect in NC3 limits the increase in RI RNA numbers at 39.5°C by inhibiting new negative-strand RNA synthesis.

DISCUSSION

The transcriptional strategy of coronaviruses is complex, and there is considerable controversy about the role of the full-length and subgenomic-length negative-strand RNAs in mRNA synthesis. While biochemical and molecular data have revealed the structure of the subgenomic mRNA, the heterogeneity within the leader-body fusion sites, and the structure of the subgenomic negative-strand RNA, very little genetic support for any of the current models for MHV transcription has been obtained. In this study, we have focused on the complementation group C mutants since previous studies have suggested that these mutants contain an early defect in RNA synthesis that probably results in a reduction in the amount of negative-strand RNA after a shift to the restrictive temperature (35).

The group C mutants are tightly linked by complementation and standard genetic recombination mapping techniques, yet the group C1 mutants synthesize mRNA and produce infectious virus after the temperature shift whereas under identical conditions the group C2 mutants are defective in the synthesis of mRNA and virus. We cannot conclusively rule out the possibility that the group C2 mutants contain a second mutation in a complementation group which is not represented within our panel of mutants. Thus, while additional experiments are needed to clearly demonstrate the presence of two noncomplementable functions within complementation group C, these findings may not be surprising, because there have been similar reports with *ts* mutants of SB HR virus (30). For example, the complementation group A mutants of SB virus map to *nsp2*, which functions in 26S mRNA synthesis, the regulation of negative-strand RNA synthesis, and proteolytic processing of the nonstructural proteins (10). These defects are present in some subgroup SB virus A1 mutants but not in the subgroup A2 mutants (10, 30). Alternatively, some group C mutants of MHV may possess a mutation in a different gene which does not complement the group C *ts* allele.

TABLE 6. Predicted MHV RNA polymerase rates at the permissive and restrictive temperatures

Template	Virus	RNA transcription rate[a] (10^3 nucleotides/min) at:	
		Permissive temp	Restrictive temp
Subgenomic	NC3	1.34 ± 0.7	1.85 ± 1.30
	NC3-Rev2	1.34 ± 1.0	1.48 ± 0.8
Full-length	NC3	14.68 ± 1.9	26.38 ± 5.8
	NC3-Rev2	15.13 ± 2.7	19.50 ± 5.9

[a] Mean ± standard deviation.

A variety of data support the hypothesis that the group C1 mutants contain a defect in the ability to synthesize full-length as well as subgenomic-length negative-strand RNA. Previous studies with strand-specific probes indicate a ~80% loss in total levels of negative-strand RNA after a shift to 39.5°C, relative to controls maintained at 32°C (35). Similarly, total RF RNA synthesis is reduced by about 83 to 92% after the shift to 39.5°C and the block in RNA synthesis prevents the accumulation of both full-length and subgenomic-length RF RNA equally. Since the rates of positive-strand synthesis at 39.5°C are at least equal to the rates of 32°C, regardless of the size of the template, the most logical conclusion is that the group C1 allele regulates negative-strand RNA synthesis.

Studies on the effect of cycloheximide on MHV RNA synthesis indicate that the negative-strand polymerase requires continuing protein synthesis, perhaps for initiation (32). The putative MHV negative-strand RNA polymerase continues to function for 1 to 2 h in the absence of protein synthesis, however, and is more resistant to cycloheximide than is the SB negative-strand RNA polymerase, which completely ceases activity after 30 min (31, 32). Slight increases in total NC3 RF RNA levels are evident after the temperature shift, suggesting that the defect in NC3 permits low levels of negative-strand RNA synthesis until the preexisting negative-strand RNA polymerase decays. SB virus *ts* mutants, defective in negative-strand synthesis, also transcribe some negative-strand RNA for approximately 1 h after the shift to the restrictive temperature (31). Alternatively, the slow increase in NC3 RF RNA labeling after the shift may be due to hotter pools of nucleotide precursors. We believe that this is unlikely, since labeling periods were identical and similar increases were not detected within the revertant virus.

Previous studies indicated that the majority (>98%) of negative-strand RNA was found in RIs in MHV-infected cells (32). It has also been shown that at 37°C, MHV negative-strand RNA synthesis peaks at 6 h p.i. and decreases thereafter, whereas positive-strand RNA synthesis continues (32). Negative-strand synthesis peaks slightly later (7 to 9 h p.i.) for *ts* mutants at 32°C, with peak RF RNA levels occurring by 9 h p.i. (35). We were able to detect full-length as well as subgenomic-length RF RNAs from 3 to 12 h p.i. at 32°C and at 39.5°C after the temperature shift late in infection (9 h p.i.). Since subgenomic RF RNA was labeled after the temperature shift late in infection, when negative-strand synthesis had terminated, these data indicated that the subgenomic negative strands were continuously functioning as templates for mRNA synthesis. This is in agreement with previous data indicating

that after negative-strand synthesis decreased, radiolabel was incorporated into RIs at a constant rate, suggesting that the MHV subgenomic negative-strand RNAs were stable (32). Similar findings have been reported with bovine coronavirus and transmissible gastroenteritis virus (11, 37).

Additional support for the idea that subgenomic negative strands are functional templates for positive-strand synthesis is demonstrated by temperature shift experiments early in infection. The decrease in total RF RNA synthesis cannot be attributed to a decrease in positive-strand synthesis, since positive-strand RNA polymerase rates significantly increase after the shift to 39.5°C. In the absence of significant amounts of new negative-strand RNA, full-length and subgenomic-length RF RNAs are also labeled at a constant rate at different times after the shift, indicating that the full-length and subgenomic-length RIs are stable and transcriptionally active throughout infection. If subgenomic negative strands are dead-end transcriptional intermediates, a reduction in the amount of radiolabel incorporated at 39.5°C into the subgenomic RFs, but not full-length RFs, should occur over time in cultures infected with *ts* mutants transcribing little new negative-strand RNA. Since this is not the case, we conclude that subgenomic-length negative- strands are functional templates for the synthesis of positive-strand RNA throughout infection, as proposed by Sethna et al. (36, 37) and Sawicki and Sawicki (33).

Our results and those of others clearly demonstrate that subgenomic negative strands are the predominant template for mRNA synthesis late in infection (33, 36, 37). Consonant with these findings, the times required for the transcription of mRNA from a subgenomic template are more in line with the times required to synthesize SB virus 26S mRNA (~2,600 nucleotides/min) as well as other previously published eukaryotic RNA polymerase rates of approximately 1,800 nucleotides/min (3, 7, 39, 41). Therefore, it appears that the subgenomic negative strands are present in sufficient quantities to act as templates for the amount of mRNA synthesized during infection. Not surprisingly, the relative percent molar ratios of mRNA and RF RNA closely parallel each other throughout infection, readily explaining the concentrations of each viral mRNA transcribed during infection. These findings are also in agreement with results of UV transcriptional mapping studies, which indicate that the UV target size for mRNA synthesis is equivalent to the size of the mRNA late in infection (12, 43). The increased rates of positive-strand synthesis from subgenomic negative strands in NC3-infected cells at 39.5°C could be due to either an increase in polymerase activity at higher temperatures or an altered ratio of positive-strand polymerase to negative-strand RNA template. Since the revertant virus had similar transcription rates at 32°C and 39.5°C, the most logical interpretation of these data is that increased transcription rates in NC3-infected cells may be attributed primarily to an altered ratio of positive-strand polymerase to negative-strand template. Under these conditions, the observed ~10-fold reduction in NC3 RF RNA template levels might result in only a ca. twofold reduction in mRNA levels after the shift. Similar findings have been reported during SB virus transcription (3).

In contrast, if leader-primed transcription from full-length negative-strand RNA is the only mechanism by which subgenomic mRNAs are synthesized, it would have to occur at a remarkable rate and efficiency. In general, polymerases with high transcription and replication rates have high processivity; i.e., they do not dissociate from the template easily (7, 39, 41). This is inconsistent with findings with MHV which suggest that nascent positive strands are found associated with and dissociated from RI RNA complexes (5) and that high-frequency RNA recombination may be mediated by a copy choice mechanism between transcriptionally active full-length and subgenomic-length RNA intermediates (2, 9, 14, 21, 24). The most logical interpretation of these data is that late in infection, subgenomic negative strands represent the major template for the synthesis of subgenomic mRNA (33, 36, 37).

The original model for MHV transcription proposed that all viral mRNAs were synthesized by a leader-primed transcription mechanism from a full-length negative-strand RNA. This model was heavily based on the observation that only a single full-length negative-strand RNA and RF RNA were present within MHV-infected cells (16) and on biochemical structural analyses of exclusion chromatography- and sucrose gradient size-purified RI RNAs (4). Although we believe that the biochemical structure of the highly purified full-length RI RNA is probably correct, since exclusion chromatography and gradient centrifugation should have removed the smaller MHV RI RNAs from the purified genome-length RI RNA (4), there is no question that subgenomic-length negative-strand RNA and RF RNAs are present, indicating that the original model must be modified. Current models for the synthesis of subgenomic negative-strand RNA include primary transcription by looping out or transcription attenuation from the genome-length template (33) and transcription from preexisting mRNA, which was initially synthesized by leader-primed transcription (32, 36, 37). Elegant studies, which strongly support the initial synthesis of subgenomic mRNAs by a leader-primed transcription model, would suggest that the newly synthesized subgenomic mRNAs act as a template for the subsequent transcription of subgenomic negative-strand RNAs containing antileaders (22, 44). However, in contrast to our results and those of others, it was suggested that neither the subgenomic-length negative-strand RNAs nor the mRNAs act as the template for transcription or replication (13, 22). These arguments are based on experiments which demonstrated that infectious defective interfering (DI) RNAs, but not mRNA, replicated and transcribed subgenomic-length mRNAs following transfection into MHV-infected cells (13, 22). Unfortunately, no compelling evidence was presented that demonstrated that the negative-strand RNAs were transcriptionally inactive templates, since highly sensitive methods to detect RI or RF RNAs were not used in these studies. Moreover, MHV DI RNAs replicate to the detriment of helper virus and have extremely high rates of transcription compared with those of other mRNA and genomic RNAs (23, 26). Within 6 h of transfection, major amounts of MHV DI RNAs were synthesized compared with SB virus DI RNAs, which were detected only after several cycles of virus passage (20). In contrast, synthesis of MHV full-length and subgenomic-length positive- and negative-strand RNA, but not DI RNAs, is clearly under tight regulatory control. Consequently, it should not be surprising that DI RNAs rapidly amplify while mRNA transcription is not readily detected under identical treatment conditions. Also, in the highly sensitive in vitro system described by Liao and Lai (22), the ability of chimeric mRNA constructs to act as a template for negative-strand RNA and similarly sized mRNA synthesis was not evaluated; only the potential for a larger chimeric mRNA to act as template for the synthesis of a smaller subgenomic mRNA encoding the chloramphenicol acetyltransferase reporter gene was discussed. Recently, mRNA transfection experiments have clearly demonstrated that in vitro transcribed mRNAs act as template for RNA recombination and repair of *ts* lesions consistent with the notion that subgenomic RNAs participate in transcription (14). Moreover, the possibility of a *cis*-acting subgenomic

negative-strand RNA polymerase cannot be excluded, nor is it clear whether transfected indicator mRNAs are compartmentalized into the appropriate viral ribonucleoprotein structures required for transcription. Alternatively, the mRNA transfection studies may support the notion that subgenomic negative-strand RNA primarily originates from genome-length template by the transcription attenuation or the looping out model (33).

Careful examination of the literature demonstrates a wealth of data supporting both an initial discontinuous transcription mechanism (4, 5, 13, 17, 22, 26, 27, 28, 34, 38) and the synthesis of mRNA from subgenomic negative strands containing antileaders (11, 33, 34, 36, 37). Since these mechanisms are not mutually exclusive but, rather, provide coronaviruses with considerable regulatory control over gene expression, the most likely interpretation is either that leader-primed transcription functions early in infection to initially transcribe mRNA, which is subsequently used as the template for the synthesis of subgenomic negative-strand RNAs or that subgenomic negative strands are synthesized directly from a genome-length template (33). The mechanism by which the subgenomic negative-strand RNAs act as template for mRNA synthesis is unknown. It has been suggested that mRNA replication occurs from subgenomic negative-strand RNAs in a manner similar to that of genome replication, since the 5′ and 3′ ends of these RNAs are identical (37). Alternative models include a *cis*-acting RNA polymerase which functions in the initial synthesis of subgenomic-length negative-strand RNA directly from newly transcribed subgenomic mRNA templates or that leader-primed transcription may also function in the synthesis of mRNA from subgenomic negative strands containing antileaders.

ACKNOWLEDGMENTS

We are grateful to Stan Sawicki for providing us with 17CL1 cells as well as valuable advice regarding the isolation of MHV RF RNAs. We also thank Lorraine Alexander, Sheila Peel, Wan Chen, and Boyd Yount for their assistance with the computer programs, technical expertise, and valuable discussion.

This research was supported by grants from the American Heart Association (AHA 901112) and the National Institutes of Health (AI-23946) and was performed during the tenure of an Established Investigator of the American Heart Association (AHA 890193) (R.S.B.).

REFERENCES

1. **Baker, S. C., and M. M. C. Lai.** 1990. An *in vitro* system for the leader-primed transcription of coronavirus mRNAs. EMBO J. **9**:4173–4179.
2. **Baric, R. S., K. S. Fu, M. C. Schaad, and S. A. Stohlman.** 1990. Establishing a genetic recombination map for MHV-A59 complementation groups. Virology **177**:646–656.
3. **Baric, R. S., D. W. Lineberger, and R. E. Johnston.** 1983. Reduced synthesis of Sindbis virus negative-strand RNA in cultures treated with host transcription inhibitors. J. Virol. **47**:46–54.
4. **Baric, R. S., S. A. Stohlman, and M. M. C. Lai.** 1983. Characterization of replicative intermediate RNA of mouse hepatitis virus: presence of leader RNA sequences on nascent chains. J. Virol. **48**: 633–640.
5. **Baric, R. S., S. A. Stohlman, M. K. Razavi, and M. M. C. Lai.** 1985. Characterization of leader-related small RNAs in coronavirus infected cells: further evidence for leader-primed mechanism of transcription. Virus Res. **3**:19–33.
6. **Budzilowicz, C. J., S. P. Wilczynski, and S. R. Weiss.** 1985. Three intergenic regions of coronavirus mouse hepatitis virus strain A59 genome RNA contain a common nucleotide sequence that is homologous to the 3′ end of the viral mRNA leader sequence. J. Virol. **53**:834–840.
7. **Chambon, P.** 1974. Eucaryotic RNA polymerases, p. 261–331. *In* P. D. Boyer (ed.), The enzymes, vol. 10. Academic Press, Inc., New York.
8. **Cheley, S., R. Anderson, M. J. Cupples, E. C. M. L. Chan, and V. L. Morris.** 1981. Intracellular murine hepatitis virus-specific RNAs contain common sequences. Virology **112**:596–604.
9. **Fu, K., and R. S. Baric.** 1992. Evidence for variable rates of recombination in the MHV genome. Virology **189**:88–102.
10. **Hahn, Y. S., E. G. Strauss, and J. H. Strauss.** 1989. Mapping of the RNA$^-$ temperature-sensitive mutants of Sindbis virus: assignment of complementation groups A, B, and G to nonstructural proteins. J. Virol. **63**:3142–3150.
11. **Hofmann, M. A., P. B. Sethna, and D. A. Brian.** 1990. Bovine coronavirus mRNA replication continues throughout persistent infection in cell culture. J. Virol. **64**:4108–4114.
12. **Jacobs, L., W. J. M. Spaan, M. C. Horzinek, and B. A. M. van der Zeijst.** 1981. Synthesis of subgenomic mRNAs of mouse hepatitis virus is initiated independently: evidence from UV transcriptional mapping. J. Virol. **39**:401–406.
13. **Jeong, Y. S., and S. Makino.** 1992. Mechanism of coronavirus transcription: duration of primary transcription initiation activity and effects of subgenomic RNA transcription on RNA replication. J. Virol. **66**:3339–3346.
14. **Koetzner, C. A., M. M. Parker, C. S. Ricard, L. S. Sturman, and P. S. Masters.** 1992. Repair and mutagenesis of the genome of a deletion mutant of the coronavirus mouse hepatitis virus by targeted RNA recombination. J. Virol. **66**:1841–1848.
15. **Lai, M. M. C., R. S. Baric, P. R. Brayton, and S. A. Stohlman.** 1984. Characterization of leader RNA sequences on the virion and mRNAs of mouse hepatitis virus, a cytoplasmic virus. Proc. Natl. Acad. Sci. USA **81**:3626–3630.
16. **Lai, M. M. C., C. D. Patton, and S. A. Stohlman.** 1982. Replication of mouse hepatitis virus: negative-stranded RNA and replicative-form RNA are of genome length. J. Virol. **44**:487–492.
17. **LaMonica, N., K. Yokomori, and M. M. C. Lai.** 1992. Coronavirus mRNA synthesis: identification of novel transcription initiation signals which are differentially regulated by different leader sequences. Virology **188**:402–407.
18. **Leibowitz, J. L., J. R. de Vries, and M. V. Haspel.** 1982. Genetic analysis of murine hepatitis virus strain JHM. J. Virol. **42**:1080–1087.
19. **Lee, H.-J., C.-K. Shieh, A. E. Gorbalenya, E. V. Koonin, N. La Monica, J. Tuler, A. Bagdzhadzhyan, and M. M. C. Lai.** 1990. The complete sequence (22 kilobases) of murine coronavirus gene 1 encoding the putative proteases and RNA polymerase. Virology **180**:567–582.
20. **Levis, R., B. G. Weiss, M. Tsiang, H. Huang, and S. Schlesinger.** 1986. Deletion mapping of Sindbis virus RNAs derived from cDNAs defines the sequences essential for replication and packaging. Cell **44**:137–145.
21. **Liao, C.-L., and M. M. C. Lai.** 1992. RNA recombination in a coronavirus: recombination between viral genomic RNA and transfected RNA fragments. J. Virol. **66**:6117–6124.
22. **Liao, C.-L., and M. M. C. Lai.** 1994. Requirement of the 5′-end genomic sequence as an upstream *cis*-acting element for coronavirus subgenomic mRNA transcription. J. Virol. **68**:4727–4734.
23. **Makino, S., M. Joo, and J. Makino.** 1991. A system for study of coronavirus mRNA synthesis: a regulated, expressed subgenomic defective interfering RNA results from intergenic site insertion. J. Virol. **65**:6031–6041.
24. **Makino, S., J. G. Keck, S. A. Stohlman, and M. M. C. Lai.** 1986. High frequency RNA recombination of murine coronaviruses. J. Virol. **57**:729–737.
25. **Makino, S., and M. M. C. Lai.** 1989. Evolution of the 5′ end of genomic RNA of murine coronaviruses during passages *in vitrol* Virology **169**:227–232.
26. **Makino, S., and M. M. C. Lai.** 1989. High-frequency leader sequence switching during coronavirus defective interfering RNA replication. J. Virol. **63**:5285–5292.
27. **Makino, S., L. H. Soe, C.-K. Shieh, and M. M. C. Lai.** 1988. Discontinuous transcription generates heterogeneity at the leader fusion sites of coronaviruses mRNAs. J. Virol. **62**:3870–3873.
28. **Makino, S., S. A. Stohlman, and M. M. C. Lai.** 1986. Leader sequences of murine coronavirus mRNAs can be freely reassorted: evidence for the role of free leader RNA in transcription. Proc. Natl. Acad. Sci. USA **83**:4204–4208.

29. **Pachuk, C. J., D. J. Bredenbeck, P. W. Zoltick, W. J. M. Spaan, and S. R. Weiss.** 1989. Molecular cloning of the gene encoding the putative polymerase of mouse hepatitis coronavirus strain A59. Virology **171**:141–148.
30. **Sawicki, D. L., and S. G. Sawicki.** 1985. Functional analysis of the A complementation group mutants of Sindbis HR virus. Virology **144**:20–34.
31. **Sawicki, D. L., S. G. Sawicki, S. Keränen, and L. Kääriäinen.** 1981. Specific Sindbis virus-coded function for minus-strand RNA synthesis. J. Virol. **39**:348–358.
32. **Sawicki, S. G., and D. L. Sawicki.** 1986. Coronavirus minus-strand RNA synthesis and effect of cycloheximide on coronavirus RNA synthesis. J. Virol. **57**:328–334.
33. **Sawicki, S. G., and D. L. Sawicki.** 1990. Coronavirus transcription: subgenomic mouse hepatitis virus replicative intermediates function in RNA synthesis. J. Virol. **64**:1050–1056.
34. **Schaad, M. C., and R. S. Baric.** 1993. Evidence for new transcriptional units encoded at the 3′ end of the mouse hepatitis virus genome. Virology **196**:190–198.
35. **Schaad, M. C., S. A. Stohlman, J. Egbert, K. Lum, K. Fu, T. Wei, Jr., and R. S. Baric.** 1990. Genetics of mouse hepatitis virus transcription: identification of cistrons which may function in positive and negative strand RNA synthesis. Virology **177**:634–645.
36. **Sethna, P. B., M. A. Hofmann, and D. A. Brian.** 1991. Minus-strand copies of replicating coronavirus mRNAs contain antileaders. J. Virol. **65**:320–325.
37. **Sethna, P. B., S.-L. Hung, and D. A. Brian.** 1989. Coronavirus subgenomic minus-strand RNAs and the potential for mRNA replicons. Proc. Natl. Acad. Sci. USA **86**:5626–5630.
38. **Shieh, C.-K., H.-J. Lee, K. Yokomori, N. LaMonica, S. Makino, and M. M. C. Lai.** 1989. Identification of a new transcriptional initiation site and the corresponding functional gene 2b in the murine coronavirus RNA genome. J. Virol. **63**:3729–3736.
39. **Simmons, D. T., and J. H. Strauss.** 1972. Replication of sindbis virus. II. Multiple forms of double-stranded RNA isolated from infected cells. J. Mol. Biol. **71**:615–631.
40. **Spaan, W., H. Delius, M. Skinner, J. Armstrong, P. Rottier, S. Smeekens, B. A. M. van der Zeijst, and S. G. Siddell.** 1983. Coronavirus mRNA synthesis involves fusion of non-contiguous sequences. EMBO J. **2**:1839–1844.
41. **Tabor, S., and C. C. Richardson.** 1987. DNA sequence analysis with a modified bacteriophage T7 DNA polymerase. Proc. Natl. Acad. Sci. USA **84**:4767–4771.
42. **Yokomori, K., L. R. Banner, and M. M. C. Lai.** 1991. Heterogeneity of gene expression of the hemagglutinin-esterase (HE) protein of murine coronaviruses. Virology **183**:647–657.
43. **Yokomori, K., L. R. Banner, and M. M. C. Lai.** 1992. Coronavirus mRNA transcription: UV light transcriptional mapping studies suggest an early requirement for a genomic-length template. J. Virol. **66**:4671–4678.
44. **Zhang, X., C.-L. Liano, and M. M. C. Lai.** 1994. Coronavirus leader RNA regulates and initiates subgenomic mRNA transcription both in *trans* and in *cis*. J. Virol. **68**:4738–4746.